

# Fractional Fokker-Planck equation and oscillatory behavior of cumulant moments

N. Suzuki

*Matsusho Gakuen Junior College, Matsumoto 390-1295, Japan*

M. Biyajima

*Department of Physics, Shinshu University, Matsumoto 390-8621, Japan*

(Received 21 January 2001; revised manuscript received 19 June 2001; published 19 December 2001)

The Fokker-Planck equation is considered, which is connected to the birth and death process with immigration by the Poisson transform. The fractional derivative in time variable is introduced into the Fokker-Planck equation in order to investigate an origin of oscillatory behavior of cumulant moments. From its solution (the probability density function), the generating function (GF) for the corresponding probability distribution is derived. We consider the case when the GF reduces to that of the negative binomial distribution (NBD), if the fractional derivative is replaced to the ordinary one. The  $H_j$  moment derived from the GF of the NBD decreases monotonically as the rank  $j$  increases. However, the  $H_j$  moment derived in our approach oscillates, which is contrasted with the case of the NBD. Calculated  $H_j$  moments are compared with those of charged multiplicities observed in  $p\bar{p}$ ,  $e^+e^-$ , and  $e^+p$  collisions. A phenomenological meaning of introducing the fractional derivative in time variable is discussed.

DOI: 10.1103/PhysRevE.65.016123

PACS number(s): 02.50.-r, 05.40.-a, 13.85.-t

## I. INTRODUCTION

The negative binomial distribution is often used for the analysis of observed multiplicity distributions in high energy hadron-hadron ( $hh$ ) and  $e^+e^-$  collisions. The cumulant moment (or the  $H_j$  moment defined by the cumulant moment normalized by the factorial moment) derived from the generating function of the negative binomial distribution (NBD) does not show oscillatory behaviors as the rank of the cumulant moment (or  $H_j$  moment) increases. On the other hand,  $H_j$  moments obtained from observed multiplicity distributions in  $hh$  and  $e^+e^-$  collisions show oscillatory behaviors [1,2]. Those behaviors can be explained if multiplicity distributions truncated at the highest observed multiplicities are used for the calculation of  $H_j$  moments. In  $hh$  collisions, calculated results from the NBD and those from the modified NBD both fit the data well [3,4]. In  $e^+e^-$  collisions, calculated  $H_j$  moments by the use of the modified NBD (MNBD) describe the oscillatory behavior of the data well. However, those by the NBD oscillate much weaker than the data, and cannot explain the behavior of the data [5].

The NBD and the MNBD are derived from the branching equations; the former is from a birth and death process with immigration, and the latter is from a pure birth (or birth and death process). In those branching equations, it is assumed that particles are produced instantaneously, in other words, without memory.

In high energy particle-particle collision processes, it is considered that a proper time is needed for a secondary produced particle to behave as an independent particle from the parent particle after the collision of the parent with a target particle [6]. In high energy hadron-nucleus or lepton-nucleus collisions, this effect should be observed as a suppression of multiplicity compared with the case of instantaneous collision, because the incident particle can collide with another target particle in the same nucleus within the proper time after the first collision. This proper time is called the formation zone [7], which means some memory effect should be

existent in the high energy particle production processes.

In the branching equations, particles are assumed to be produced successively. If a memory effect is introduced into the branching process, it will be very interesting what results come out.

The birth and death process with immigration is described by the following equation:

$$\frac{\partial P(n,t)}{\partial t} = \lambda_0 [P(n-1,t) - P(n,t)] + \lambda_2 [(n-1)P(n-1,t) - nP(n,t)] + \lambda_1 [(n+1)P(n+1,t) - nP(n,t)], \quad (1)$$

where  $P(n,t)$  denotes the probability distribution that  $n$  particles are existent at time  $t$ ,  $\lambda_0$  denotes an immigration rate,  $\lambda_1$  a death rate, and  $\lambda_2$  a birth rate. If the initial condition is taken as

$$P(n,t=0) = \delta_{n,0},$$

the solution of Eq. (1) becomes the NBD.

The probability density function, Koba-Nielsen-Olesen (KNO) scaling function  $\psi(z,t)$  is connected to the probability distribution (multiplicity distribution)  $P(n,t)$  by the Poisson transform,

$$P(n,t) = \frac{\langle n_0 \rangle^n}{n!} \int_0^\infty z^n \exp[-\langle n_0 \rangle z] \psi(z,t) dz. \quad (2)$$

The KNO scaling function  $\psi(z,t)$  is obtained from the multiplicity distribution  $P(n,t)$  by the inverse Poisson transform,

$$\psi(z,t) = \frac{\langle n_0 \rangle}{2\pi\alpha} \exp[\langle n_0 \rangle z] \int_{-\infty}^{\infty} \sum_{n=0}^{\infty} \left(\frac{ix}{\alpha}\right)^n P(n,t) \times \exp\left[-ix \frac{\langle n_0 \rangle}{\alpha} z\right] dx. \quad (3)$$

Applying the inverse Poisson transform (3) to Eq. (1), we obtain the Fokker-Planck equation,

$$\frac{\partial \psi(z,t)}{\partial t} = -\frac{\partial}{\partial z} \left[ a(z) - \frac{1}{2} \frac{\partial}{\partial z} b(z) \right] \psi(z,t), \quad (4)$$

where

$$a(z) = \beta - \gamma z, \quad b(z) = \sigma^2 z, \quad \beta = \frac{\lambda_0}{\langle n_0 \rangle}, \quad \gamma = \lambda_1 - \lambda_2, \quad \sigma^2 = \frac{2\lambda_2}{\langle n_0 \rangle}. \quad (5)$$

In Eq. (5),  $\beta > 0$ ,  $\sigma^2 > 0$ , and  $\gamma$  is real. If time derivative in Eq. (4) is replaced to the fractional one, we have reached to the fractional Fokker-Planck equation in time variable as a model for high energy particle production processes, in which a memory effect is taken into account.

The fractional calculus has been investigated for hundreds of years [8,9]. Recently, the fractional Fokker-Planck equation in time variable was derived from the continuous time random walk [10]. It is applied to the analysis of anomalous diffusion phenomena [11]. The fractional derivative in space variable is introduced into the Fokker-Planck equation to describe the Lévy process [12].

We would take the fractional Fokker-Planck equation in time variable corresponding to the branching equation (1) as a model for particle production processes, and to investigate it's solution, which reduces to the  $\gamma$  distribution when the fractional derivative is replaced to the ordinary one. We also examine the effect of fractional derivative or introducing the memory effect on the behavior of cumulant moments.

## II. A MODEL FOR PARTICLE PRODUCTION PROCESSES

The fractional Fokker-Planck equation (FFPE),

$$\frac{\partial \psi(z,t)}{\partial t} = {}_0\mathcal{D}_t^{1-\alpha} \mathcal{L}_{\text{FP}} \psi(z,t), \quad 0 < \alpha < 1, \quad \mathcal{L}_{\text{FP}} = -\frac{\partial}{\partial z} \left[ a(z) - \frac{1}{2} \frac{\partial}{\partial z} b(z) \right], \quad (6)$$

with the initial condition,

$$\psi(z,t=0) = \delta(z-z_0), \quad z_0 > 0, \quad (7)$$

is taken as a model for particle production processes. In Eq. (6),  ${}_0\mathcal{D}_t^\delta$  denotes the Riemann-Liouville fractional derivative [8,9]. The derivation of  $\psi(z,t)$  from Eq. (6) is shown in Appendix A.

In the limit of  $z_0 \rightarrow +0$ , the solution of Eq. (6) for  $\gamma > 0$  reduces to

$$\psi(z,t) = \frac{1}{\Gamma(\lambda)} \frac{z^{\lambda-1}}{k^\lambda} \exp\left[-\frac{z}{k}\right] \sum_{m=0}^{\infty} L_m^{(\lambda-1)}\left(\frac{z}{k}\right) E_\alpha(-m\gamma t^\alpha), \quad (8)$$

where  $E_\alpha(-t)$  denotes the Mittag-Leffler function. If  $\alpha = 1$ , Eq. (8) coincides with the  $\gamma$  distribution, the KNO scaling function of the NBD.

The generating function (GF) for the multiplicity distribution corresponding to the KNO scaling function, Eq. (8), is derived in Appendix B, where the  $j$ th rank normalized factorial moment and a formula for the  $H_j$  moment are obtained from the GF. The normalized factorial moment is given by

$$F_j = \frac{f_j}{\langle n \rangle^j} = \frac{\Gamma(\lambda+j)}{\Gamma(\lambda)\lambda^j} \frac{\sum_{m=0}^j (-1)^m {}_j C_m E_\alpha(-m\gamma t^\alpha)}{[1-E_\alpha(-\gamma t^\alpha)]^j}. \quad (9)$$

The recurrence equation for the  $H_j$  moment is written as

$$H_1 = 1, \quad H_j = 1 - \sum_{m=1}^{j-1} {}_{j-1} C_{m-1} \frac{F_{j-m} F_m}{F_j} H_m. \quad (10)$$

The normalized factorial moment and the  $H_j$  moment for the NBD are given respectively as,

$$F_{\text{NBD},j} = \frac{\Gamma(\lambda+j)}{\Gamma(\lambda)\lambda^j}, \quad (11)$$

$$H_{\text{NBD},j} = \frac{\Gamma(\lambda+1)(j-1)!}{\Gamma(\lambda+j)}. \quad (12)$$

As can be seen from Eqs. (9) and (11), difference between the normalized factorial moment derived from the FFPE ( $0 < \alpha < 1$ ) and that of the NBD ( $\alpha = 1$ ) is given by Mittag-Leffler functions.

We can see from Eq. (A15) in Appendix A that

$$\lim_{t \rightarrow +\infty} E_\alpha(-\gamma t^\alpha) = 0.$$

Then,  $F_j$  moment given by Eq. (9) coincides with  $F_{\text{NBD},j}$  in Eq. (11) in the limit of  $t \rightarrow +\infty$ . Therefore,  $H_j$  moment calculated from Eq. (9) also coincides with  $H_{\text{NBD},j}$  in the same time limit.

## III. CALCULATED RESULTS

At first, calculated results of the Mittag-Leffler function  $E_\alpha(-t)$  is shown in Fig. 1. It is a decreasing function of variable  $t$ , and as  $\alpha$  increases from 0 to 1, it decreases more faster as a function of variable  $t$ .

In the following calculations, observed values of  $\langle n \rangle$  and  $C^2 (= \langle n^2 \rangle / \langle n \rangle^2)$  for the charged particles are used. Then, if  $\alpha$  and  $\gamma t^\alpha$  are given,  $\lambda$  in Eq. (9) is determined by the following equation:

$$\frac{1}{\lambda} = \left( C^2 - \frac{1}{\langle n \rangle} \right) \frac{[1-E_\alpha(-\gamma t^\alpha)]^2}{1-2E_\alpha(-\gamma t^\alpha)+E_\alpha(-2\gamma t^\alpha)} - 1.$$

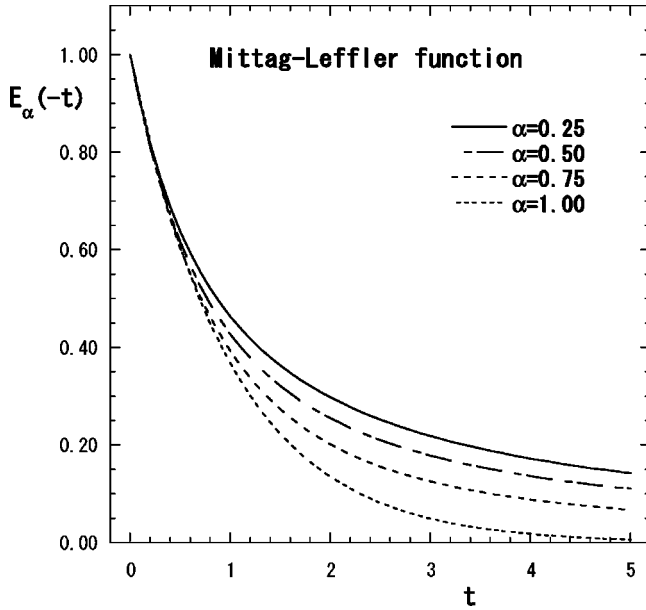


FIG. 1. The Mittag-Leffler function calculated from Eq. (A15) with  $\alpha=0.25, 0.50, 0.75,$  and  $1.00$ .

In order to see the effect of the fractional derivative, i.e.,  $0 < \alpha < 1$ , to the oscillatory behavior of  $H_j$  moments, calculated  $H_j$  moments are shown in Fig. 2(a) with  $\alpha=0.25$ , and  $\gamma t^\alpha=1.5, 2.0,$  and  $2.5$ , in Fig. 2(b) with  $\alpha=0.50$ , and  $\gamma t^\alpha=1.0, 1.5,$  and  $2.0$ , and in Fig. 2(c) with  $\alpha=0.75$ , and  $\gamma t^\alpha=0.5, 1.0,$  and  $1.5$ . In our calculation,  $\langle n \rangle = 29.2$  and  $C^2 = 1.274$ , observed values in  $p\bar{p}$  collisions at  $\sqrt{s} = 546$  GeV, are used [14]. If  $\alpha$  is fixed, oscillation of the  $H_j$  moment as a function of rank  $j$  becomes weaker as the value of parameter  $\gamma t^\alpha$  increases. If  $\gamma t^\alpha$  is fixed, oscillation of  $H_j$  moments become much weaker as  $\alpha$  increases from 0 to 1.

In Fig. 3, our calculation with  $\alpha=0.5$  and  $\gamma t^\alpha=2.23$  is compared with the  $H_j$  moment obtained from the data in  $p\bar{p}$  collisions at  $\sqrt{s} = 546$  GeV [14]. Parameter  $\gamma t^\alpha$  is adjusted with a step of 0.01 so that the first relative minimum of the calculated  $H_j$  moment should be located near the rank of that obtained from the data as much as possible. The calculated first relative minimum value is  $H_7 = -3.32 \times 10^{-5}$ , and the absolute value of it is much smaller than that obtained from the data. However, we can see from Figs. 2(b) and 3, the calculated  $H_j$  moment with  $\alpha=0.5$  and  $\gamma t^\alpha=1.0$  oscillates as strong as that from the data.

In Fig. 4, the calculated  $H_j$  moment with  $\alpha=0.5$  and  $\gamma t^\alpha=90.0$  is compared with that obtained from the data in  $e^+e^-$  collisions at  $\sqrt{s} = 91$  GeV [15]. As can be seen from the figure, the calculated value of the first relative minimum is almost the same with the data, and the strength of the oscillation of calculated  $H_j$  moment is comparable with the data.

The  $H_j$  moment in  $e^+p$  collisions in the pseudorapidity range<sup>1</sup>  $1 < \eta < 5$  in the interval  $185 < W < 220$  GeV [16] is

<sup>1</sup>Pseudorapidity  $\eta$  is defined as  $\eta = -\ln \tan(\theta/2)$ , with the polar angle of a particle.

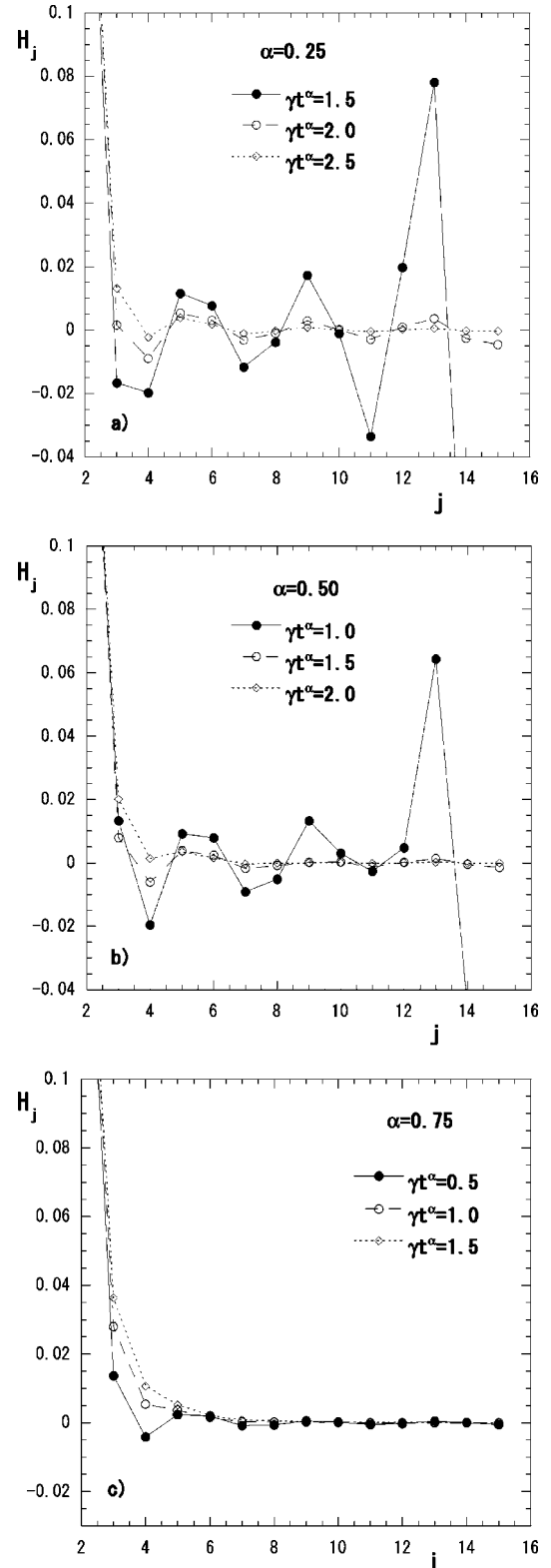


FIG. 2. Calculated results of  $H_j$  moments as a function of rank  $j$ ; (a) with  $\alpha=0.25$ , and  $\gamma t^\alpha=1.5$  ( $\lambda=48.44$ ),  $2.5$  ( $16.93$ ), and  $3.5$  ( $11.61$ ); (b) with  $\alpha=0.50$ , and  $\gamma t^\alpha=1.0$  ( $\lambda=66.82$ ),  $1.5$  ( $15.41$ ), and  $2.0$  ( $10.24$ ); (c) with  $\alpha=0.75$ , and  $\gamma t^\alpha=0.5$  ( $\lambda=20.41$ ),  $1.0$  ( $10.20$ ), and  $1.5$  ( $7.65$ ). In each calculation,  $\langle n \rangle = 29.2$  and  $C^2 = 1.274$ , observed values of charged particles in  $p\bar{p}$  collisions at  $\sqrt{s} = 546$  GeV/c [14] are used.

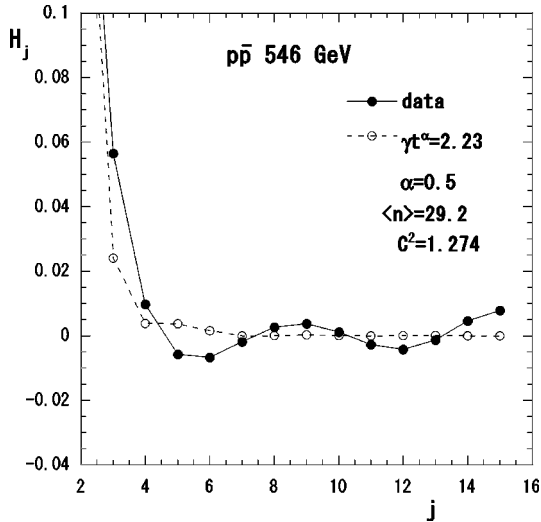


FIG. 3. Calculated result with  $\alpha=0.5$  and  $\gamma t^\alpha=2.23$  ( $\lambda=9.16$ ) is compared with the data of charged particles in  $p\bar{p}$  collisions at  $\sqrt{s}=546$  GeV/c [14], where  $\langle n \rangle=29.2$  and  $C^2=1.274$  are used. Parameter  $\alpha$  is fixed at 0.5, and  $\gamma t^\alpha$  is adjusted so that the first relative minimum of the calculated  $H_j$  moment is located at  $j \geq 5$  ( $j=7$ ).

also analyzed, and the results are shown in Fig. 5. Calculated  $H_j$  moment with  $\alpha=0.5$  and  $\gamma t^\alpha=11.2$  ( $\lambda=20.00$ ) well reproduces the first relative minimum of the data. For comparison, the  $H_j$  moment calculated with the NBD, Eq. (B11) truncated at the highest observed charged multiplicity is also shown. The parameters of the truncated NBD are determined by the minimum  $\chi^2$  fit with the observed charged multiplicity distribution. The first relative minimum of the calculated  $H_j$  moment with the truncated NBD is  $H_5 = -3.42 \times 10^{-3}$  that is different from the first relative minimum  $H_3 = -4.07 \times 10^{-3}$  obtained from the experimental data. However, the strength of the oscillation of  $H_j$  moments cal-

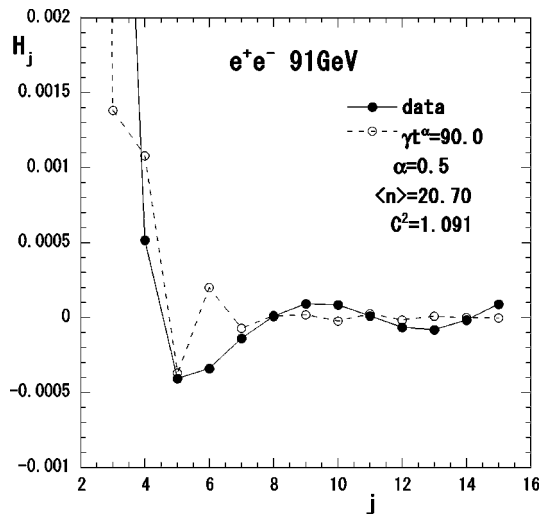


FIG. 4. Calculated  $H_j$  moments with  $\alpha=0.50$  and  $\gamma t^\alpha=90.0$  ( $\lambda=25.36$ ), as a function of rank  $j$  are compared with those in  $e^+e^-$  collisions at  $\sqrt{s}=91$  GeV/c [15].  $\langle n \rangle=20.70$  and  $C^2=11.091$  are used in our calculation.

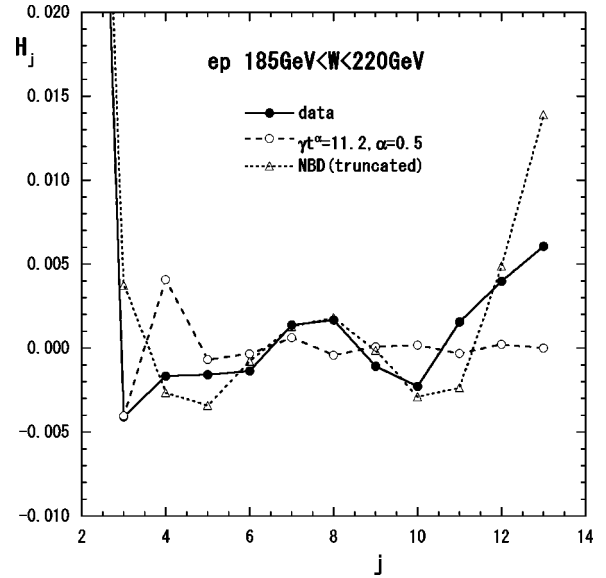


FIG. 5. Calculated  $H_j$  moments as a function of rank  $j$  are compared with the data in  $e^+p$  collisions in the pseudorapidity range  $1 < \eta < 5$  in the interval  $185 < W < 220$  GeV [16]. White circles denote the calculated result with  $\alpha=0.50$  and  $\gamma t^\alpha=11.2$ , where  $\langle n \rangle=8.80$  and  $C^2=1.190$  are used. White triangles show the  $H_j$  moment calculated with the NBD that is truncated at  $n=21$ , the highest observed charged multiplicity, where  $\langle n_b \rangle=8.825$  and  $\lambda=13.21$  are used.

culated with the truncated NBD is comparable with the data.

Estimation of  $H_j$  moment is obtained by the use of Eq. (10) from the  $F_j$  moment both in the theoretical calculation and in the calculation from the experimental data. In order to see the relation between the behavior of the  $H_j$  moment and that of the normalized factorial moment  $F_j$  as a function of rank  $j$ , we also analyze the  $F_j$  moment in  $e^+p$  collisions in the pseudorapidity range  $1 < \eta < 5$  in the interval  $185 < W < 220$  GeV [16]. The parameters are the same with those in Fig. 5. The  $F_j$  moment calculated with Eq. (9) is compared with the data in Fig. 6(a). Our calculated result in the normalized factorial moment well reproduces the experimental data up to the fourth rank. The difference between them is less than 1%. However, we cannot reproduce the fourth rank  $H_j$  moment of the data from our calculation. This result indicates that the oscillation of the  $H_j$  moment is very sensitive to the value of  $F_j$  moments.

To see the effect of truncation for the normalized factorial moment  $F_j$ , those calculated with Eq. (11) (without truncation) and with the truncated NBD are shown in Fig. 6(b). The former is calculated with  $\langle n \rangle=8.80$  and  $C^2=1.190$ . Parameters of the truncated NBD are the same with those in Fig. 5. The  $F_j$  moment with truncation is much more suppressed than that without truncation at higher rank  $j$ .

From Figs. 6(a) and 6(b), we can see that the  $F_j$  moment calculated from the FFPE is smaller than that with Eq. (11) (without truncation). Therefore, introduction of the fractional derivative in time variable suppresses the value of  $F_j$  moment compared with that of Eq. (11) as the rank  $j$  increases, and gives rise to similar effect as in truncation of multiplicity distribution.

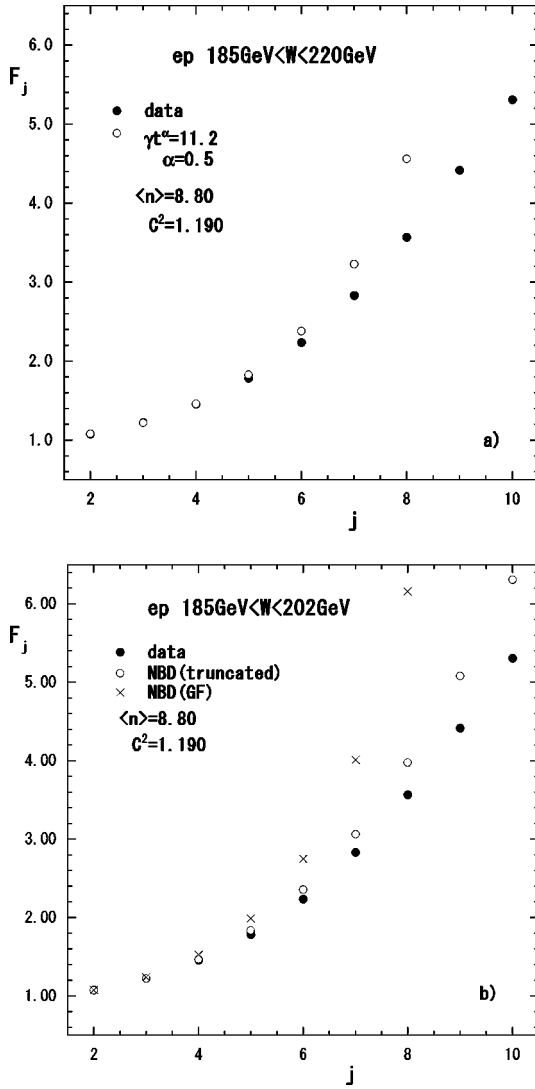


FIG. 6. Calculated normalized factorial moments  $F_j$  as a function of rank  $j$  are compared with the data in  $e^+p$  collisions in  $1 < \eta < 5$  in the interval  $185 < W < 220$  GeV [16]. (a) White circles denote the calculated result with  $\alpha = 0.50$  and  $\gamma t^\alpha = 11.2$  ( $\lambda = 20.00$ ), and black circles are the data. (b) White circles denote the result calculated with the NBD that is truncated at  $n = 21$ , where  $\langle n_b \rangle = 8.825$  and  $\lambda = 13.21$  are used. Crosses show calculated  $H_j$  moment with Eq. (11), where  $\lambda = 13.10$  is used.

The  $H_j$  moments and normalized factorial moments in  $e^+p$  collisions in  $1 < \eta < 5$  in the interval  $185 < W < 220$  GeV [16] are also calculated with sets of parameters,  $\alpha = 0.25$  and  $\gamma t^\alpha = 16.0$  ( $\lambda = 19.94$ ), or  $\alpha = 0.75$  and  $\gamma t^\alpha = 5.70$  ( $\lambda = 20.41$ ). The results become almost the same with those shown in Figs. 5 and 6.

Observed charged multiplicity distributions in the pseudorapidity windows,  $1 < \eta < \eta_m$ ,  $\eta_m = 2, 3, 4$ , and  $5$ , are also given in  $e^+p$  collisions in the interval  $185 < W < 220$  GeV [16]. We also analyze the factorial moment of multiplicities in each pseudorapidity window using the formulas given by Eq. (B6) or Eq. (9) with  $\alpha = 0.5$ . Formula of average charged multiplicity

$$\langle n \rangle = \lambda k \langle n_0 \rangle [1 - E_\alpha(-\gamma t^\alpha)], \quad (13)$$

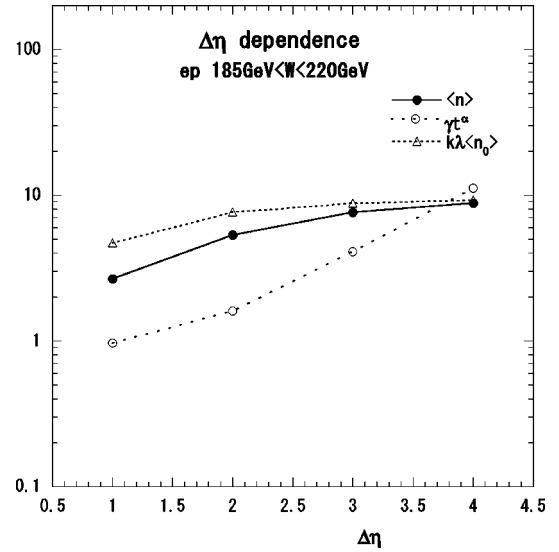


FIG. 7. Pseudorapidity window  $\Delta \eta$  dependence of  $\gamma t^\alpha$  ( $\alpha = 0.50$ ) and  $k \lambda \langle n_0 \rangle$  in  $e^+p$  collisions in the interval  $185 < W < 220$  GeV [16]. Those values are estimated from the observed average charged multiplicity  $\langle n \rangle$  in the pseudorapidity window  $\Delta \eta$  ( $\Delta \eta = \eta_m - 1$ ,  $\eta_m = 2, 3, 4, 5$ ) [16] by the use of Eq. (13).

is applied to that of the window,  $1 < \eta < \eta_m$ , which is specified by  $\Delta \eta = \eta_m - 1$ . Estimated value of  $\gamma t^\alpha$  and  $k \lambda \langle n_0 \rangle$  are shown in Fig. 7. Roughly speaking,  $\gamma t^\alpha$  increases exponentially with  $\Delta \eta$ ,

$$\gamma t^\alpha \sim \exp[0.83 \Delta \eta],$$

and  $k \lambda \langle n_0 \rangle$  increases with  $\Delta \eta$  more slowly.

#### IV. CONCLUDING REMARKS

The FFPE corresponding to the birth and death process with immigration is taken as a model for particle production processes with a memory effect. It is solved according to the procedure proposed by Barkai and Silbey [11]. From the solution of the FFPE, we obtain the generating function for the multiplicity distribution, where parameter  $\alpha$  connected with the fractional time derivative is contained. If  $\alpha$  is put to 1, the distribution becomes the NBD.

The normalized factorial moment  $F_j$  calculated with Eq. (9) becomes much smaller than that with Eq. (11) obtained from the GF for the NBD as the rank  $j$  increases, where Eq. (9) coincides with Eq. (11) if  $\alpha = 1$ . This fact means that the high multiplicity component in the multiplicity distribution is suppressed if  $\alpha < 1$ , compared with the NBD ( $\alpha = 1$ ) with the same  $\langle n \rangle$  and  $C^2$ .

When  $\alpha$  is less than 1, the oscillation of  $H_j$  moment appears, and as  $\alpha$  decreases from 1 to 0, the oscillation becomes much stronger. This is caused by the fact that the fractional derivative ( $0 < \alpha < 1$ ) is introduced into the time derivative in Eq. (6). It can be said that introducing the fractional derivative gives similar effect on the normalized factorial moment and the  $H_j$  moment as in the truncation of multiplicity distributions.

If  $\alpha$  is fixed, as can be seen from Fig. 1, the oscillation of

$H_j$  moments become weaker as  $\gamma t^\alpha$  increases. The first relative minimums of  $H_j$  moments obtained from the data are about  $-6.7 \times 10^{-3}$  in  $p\bar{p}$  collisions,  $-4.1 \times 10^{-3}$  in  $ep$  collisions, and  $-4.1 \times 10^{-4}$  in  $e^+e^-$  collisions. We have analyzed the data with  $\alpha=0.5$ . Estimated values of  $\gamma t^\alpha$  from the data are 2.23 (or 1.0), 11.2, and 90.0, respectively. The result of our analysis is consistent with the general features of  $H_j$  moments shown in Fig. 1.

**ACKNOWLEDGMENT**

One of the authors (M.B.) is partially supported by a Grant-in-Aid for Scientific Research from the Ministry of Education, Science, Sports, and Culture (Grant No. 09440103).

**APPENDIX A: FRACTIONAL FOKKER-PLANCK EQUATION**

We consider the FFPE,

$$\frac{\partial \psi(z,t)}{\partial t} = {}_0\mathcal{D}_t^{1-\alpha} \mathcal{L}_{\text{FP}} \psi(z,t), \quad 0 < \alpha < 1,$$

$$\mathcal{L}_{\text{FP}} = -\frac{\partial}{\partial z} \left[ a(z) - \frac{1}{2} \frac{\partial}{\partial z} b(z) \right], \quad (\text{A1})$$

with the initial condition

$$\psi(z,t=0) = \delta(z-z_0), \quad z_0 > 0. \quad (\text{A2})$$

In Eq. (A1), coefficients  $a(z)$  and  $b(z)$  are given by Eq. (4).  ${}_0\mathcal{D}_t^\delta$  denotes the Riemann-Liouville fractional derivative [8,9] defined by

$${}_0\mathcal{D}_t^\delta f(t) = \frac{1}{\Gamma(n-\delta)} \frac{d^n}{dt^n} \int_0^t (t-\tau)^{n-\delta-1} f(\tau) d\tau, \quad n-1 \leq \delta < n, \quad (\text{A3})$$

where  $n$  is a positive integer. If  $\alpha=1$ , Eq. (A1) reduces to Eq. (4).

According to the method proposed by Barkai and Silbey [11], we assume that

$$\psi(z,t) = \int_0^\infty R_s(t) G_s(z) ds, \quad (\text{A4})$$

and that function  $G_s(z)$  satisfies the following equations:

$$\begin{aligned} \mathcal{L}_{\text{FP}} G_s(z) &= \frac{\partial}{\partial s} G_s(z), \\ G_0(z) &= \delta(z-z_0). \end{aligned} \quad (\text{A5})$$

Then function  $G_s(z)$  is given as

$$\begin{aligned} G_s(z) &= \frac{1}{kp} \exp \left[ -\frac{z+z_0(1-p)}{kp} \right] \left( \frac{z}{z_0(1-p)} \right)^{(\lambda-1)/2} \\ &\quad \times I_{\lambda-1} \left[ \frac{2\sqrt{zz_0(1-p)}}{kp} \right], \end{aligned} \quad (\text{A6})$$

where  $\lambda > 0$ , and  $k$  and  $p$  are real; those are written respectively as,

$$\lambda = \frac{2\beta}{\sigma^2}, \quad k = \frac{\sigma^2}{2\gamma}, \quad p = 1 - e^{-\gamma s}. \quad (\text{A7})$$

Coefficient  $\lambda$  is positive. In the following, we assume that  $\gamma = \lambda_1 - \lambda_2 > 0$ . Therefore, coefficient  $k$  becomes positive. Equation (A6) can be expanded as

$$\begin{aligned} G_s(z) &= \frac{1}{k} \left( \frac{z}{k} \right)^{\lambda-1} \exp \left[ -\frac{z}{k} \right] \sum_{m=0}^\infty \frac{m!}{\Gamma(m+\lambda)} \\ &\quad \times L_m^{(\lambda-1)} \left( \frac{z}{k} \right) L_m^{(\lambda-1)} \left( \frac{z_0}{k} \right) \exp[-m\gamma s], \end{aligned} \quad (\text{A8})$$

where  $L_m^{(\lambda-1)}(z)$  denotes the Laguerre polynomial.

Applying the Laplace transform to Eq. (A1), we find

$$\begin{aligned} \int_0^\infty \left[ u \tilde{R}_s(u) + u^{1-\alpha} \frac{\partial \tilde{R}_s(u)}{\partial s} \right] G_s(z) ds \\ = [1 - u^{1-\alpha} \tilde{R}_0(u)] \delta(z-z_0), \end{aligned} \quad (\text{A9})$$

where  $\tilde{R}_s(u)$  is the Laplace transform of  $R_s(t)$ ,

$$\tilde{R}_s(u) = \int_0^\infty R_s(t) e^{-ut} dt. \quad (\text{A10})$$

Furthermore, we assume that each side of Eq. (A9) is equal to zero

$$u^{1-\alpha} \tilde{R}_0(u) = 1, \quad -u^{1-\alpha} \frac{\partial \tilde{R}_s(u)}{\partial s} = u \tilde{R}_s(u). \quad (\text{A11})$$

The solution of Eq. (A11) is given by

$$\tilde{R}_s(u) = u^{\alpha-1} \exp[-su^\alpha]. \quad (\text{A12})$$

Then  $R_s(t)$ , the inverse Laplace transform of  $\tilde{R}_s(u)$ , is written as

$$\begin{aligned} R_s(t) &= \frac{1}{2\pi i} \int_{c_0-i\infty}^{c_0+i\infty} \tilde{R}_s(u) e^{ut} du = \frac{t^{-\alpha}}{2\pi i} \int_{c_0-i\infty}^{c_0+i\infty} \sigma^{\alpha-1} \\ &\quad \times \exp \left[ \sigma - \frac{s}{t^\alpha} \sigma^\alpha \right] d\sigma \quad (c_0 > 0). \end{aligned} \quad (\text{A13})$$

Therefore, the solution of the FFPE (A1) is given by

$$\begin{aligned} \psi(z,t) &= \int_0^\infty R_s(t) G_s(z) ds = \frac{z^{\lambda-1}}{k^\lambda} \exp\left[-\frac{z}{k}\right] \sum_{m=0}^\infty \frac{m!}{\Gamma(m+\lambda)} \\ &\quad \times L_m^{(\lambda-1)}\left(\frac{z}{k}\right) L_m^{(\lambda-1)}\left(\frac{z_0}{k}\right) E_\alpha(-m\gamma t^\alpha), \end{aligned} \quad (\text{A14})$$

where  $E_\alpha(-t)$  for  $t>0$  denotes the Mittag-Leffler function of ordered  $\alpha$  [13],

$$\begin{aligned} E_\alpha(-t) &= \frac{\sin(\alpha\pi)}{\alpha\pi} \int_0^\infty \exp[-(xt)^{1/\alpha}] \\ &\quad \times \frac{1}{x^2 + 2x \cos(\alpha\pi) + 1} dx. \end{aligned} \quad (\text{A15})$$

It is written in the infinite series as

$$E_\alpha(z) = \sum_{n=0}^\infty \frac{z^n}{\Gamma(\alpha n + 1)}. \quad (\text{A16})$$

In the limit of  $z_0 \rightarrow +0$ , Eq. (A14) reduces to

$$\psi(z,t) = \frac{1}{\Gamma(\lambda)} \frac{z^{\lambda-1}}{k^\lambda} \exp\left[-\frac{z}{k}\right] \sum_{m=0}^\infty L_m^{(\lambda-1)}\left(\frac{z}{k}\right) E_\alpha(-m\gamma t^\alpha). \quad (\text{A17})$$

If  $\alpha=1$ , Eq. (A17) coincides with the  $\gamma$  distribution, the KNO scaling function of the NBD.

We have considered the FFPE for  $\gamma = \lambda_1 - \lambda_2 > 0$ , where the birth rate  $\lambda_2$  is less than the immigration rate  $\lambda_1$ . In the case for  $\gamma < 0$ , the solution of the FFPE (A1) in the limit of  $z_0 \rightarrow +0$ , is given by

$$\psi(z,t) = \frac{1}{\Gamma(\lambda)} \frac{z^{\lambda-1}}{|k|^\lambda} \sum_{m=0}^\infty L_m^{(\lambda-1)}\left(\frac{z}{|k|}\right) E_\alpha[-(m+\lambda)|\gamma|t^\alpha].$$

If  $\alpha=1$ , the above equation coincides with the  $\gamma$  distribution. However, we cannot calculate the factorial moment from it, because the exponential damping factor in  $z$  variable is not contained in the equation, contrary to Eq. (A17).

## APPENDIX B: GENERATING FUNCTION AND FACTORIAL MOMENT

The GF for the multiplicity distribution  $P(n,t)$  is defined as

$$\Pi(u) = \sum_{n=0}^\infty P(n,t) u^n. \quad (\text{B1})$$

The multiplicity distribution and the  $j$ th rank factorial moment are given from Eq. (B1), respectively, as

$$P(n,t) = \frac{1}{n!} \left. \frac{\partial^n \Pi(u)}{\partial u^n} \right|_{u=0},$$

$$\begin{aligned} f_j &= \langle n(n-1) \cdots (n-j+1) \rangle \\ &= \left. \frac{\partial^j \Pi(u)}{\partial u^j} \right|_{u=1} \\ &= \sum_{n=j}^\infty n(n-1) \cdots (n-j+1) P(n). \end{aligned} \quad (\text{B2})$$

From Eqs. (2) and (B1), the GF is written by the use of the Laplace transform of the KNO scaling function  $\psi(z,t)$  as

$$\Pi(1-u/\langle n_0 \rangle) = \int_0^\infty \psi(z,t) e^{-uz} dz. \quad (\text{B3})$$

Then the GF corresponding to Eq. (A17) is given as

$$\Pi(u) = \sum_{m=0}^\infty \frac{\Gamma(m+\lambda)}{m! \Gamma(\lambda)} \frac{[-k\langle n_0 \rangle(u-1)]^m}{[1-k\langle n_0 \rangle(u-1)]^{m+\lambda}} E_\alpha(-m\gamma t^\alpha). \quad (\text{B4})$$

The multiplicity distribution and the factorial moment are given from Eqs. (B2) and (B4), respectively, as

$$\begin{aligned} P(n,t) &= \sum_{m=0}^\infty \sum_{l=0}^{\min(m,n)} \frac{(-1)^l \Gamma(m+n+\lambda-l)}{\Gamma(\lambda)(m-l)!(n-l)! l!} \\ &\quad \times \frac{(k\langle n_0 \rangle)^{m+n-l}}{(1+k\langle n_0 \rangle)^{m+n+\lambda-l}} E_\alpha(-m\gamma t^\alpha), \end{aligned} \quad (\text{B5})$$

$$f_j = (k\langle n_0 \rangle)^j \frac{\Gamma(\lambda+j)}{\Gamma(\lambda)} \sum_{m=0}^j (-1)^m {}_j C_m E_\alpha(-m\gamma t^\alpha). \quad (\text{B6})$$

The  $j$ th rank normalized factorial moment is given by

$$F_j = \frac{f_j}{\langle n \rangle^j} = \frac{\Gamma(\lambda+j)}{\Gamma(\lambda)\lambda^j} \frac{\sum_{m=0}^j (-1)^m {}_j C_m E_\alpha(-m\gamma t^\alpha)}{[1-E_\alpha(-\gamma t^\alpha)]^j}. \quad (\text{B7})$$

The  $k$ th rank cumulant moment is defined by the following equation:

$$\kappa_j = \left. \frac{\partial^j \ln \Pi(u)}{\partial u^j} \right|_{u=1}. \quad (\text{B8})$$

From Eqs. (B6), (B7), and (B8), we obtain a recurrence equation for the  $H_j$  moment,

$$H_1 = 1, \quad H_j = 1 - \sum_{m=1}^{j-1} {}_{j-1} C_{m-1} \frac{F_{j-m} F_m}{F_j} H_m, \quad (\text{B9})$$

where

$$H_j = \kappa_j / f_j.$$

If  $\alpha = 1$ , Eq. (B4) reduces to the generating function for the NBD with mean multiplicity  $\langle n_b \rangle = k\lambda \langle n_0 \rangle (1 - e^{-\gamma t})$ ,

$$\Pi_{\text{NB}}(u) = \left[ 1 - \frac{\langle n_b \rangle}{\lambda} (u - 1) \right]^{-\lambda}. \quad (\text{B10})$$

From Eq. (B10), the NBD is given as

$$P(n, t) = \frac{\Gamma(\lambda + n)}{\Gamma(\lambda)\Gamma(n + 1)} \frac{(\langle n_b \rangle / \lambda)^n}{(1 + \langle n_b \rangle / \lambda)^{n + \lambda}}. \quad (\text{B11})$$

The normalized factorial moment and the  $H_j$  moment for the NBD are given, respectively, as

$$F_{\text{NB},j} = \frac{\Gamma(\lambda + j)}{\Gamma(\lambda)\lambda^j}, \quad H_{\text{NB},j} = \frac{\Gamma(\lambda + 1)(j - 1)!}{\Gamma(\lambda + j)}. \quad (\text{B12})$$

- 
- [1] I.M. Dremin and V.A. Nechitailo, JETP Lett. **58**, 881 (1993); I.M. Dremin and R. Hwa, Phys. Rev. D **49**, 5805 (1994).
- [2] I.M. Dremin *et al.*, Phys. Lett. B **336**, 119 (1994).
- [3] N. Nakajima, M. Biyajima, and N. Suzuki, Phys. Rev. D **54**, 4333 (1996).
- [4] R. Ugoccioni, A. Giovannini, and S. Lupia, Phys. Lett. B **342**, 387 (1995).
- [5] N. Suzuki, M. Biyajima, and N. Nakajima, Phys. Rev. D **53**, 3582 (1996); **54**, 3653 (1996).
- [6] L.D. Landau and I.Y. Pomeranchuk, Dokl. Akad. Nauk Arm. SSR **92**, 535,735 (1953); A.B. Migdal, Phys. Rev. **103**, 1811 (1956).
- [7] A. Bialas, Z. Phys. C: Part. Fields **26**, 301 (1984).
- [8] K.B. Oldham and J. Spanier, *The Fractional Calculus* (Academic Press, New York, 1974).
- [9] I. Podlubny, *Fractional Differential Equations* (Academic Press, San Diego, 1999).
- [10] E. Barkai, R. Metzler, and J. Klafter, Phys. Rev. E **61**, 132 (2000); R. Metzler and J. Klafter, *ibid.* **61**, 6308 (2000).
- [11] E. Barkai and R.J. Silbey, e-print cond-mat/0002020; R. Metzler, E. Barkai, and J. Klafter, Phys. Rev. Lett. **82**, 3563 (1999).
- [12] B.J. West, P. Grigolini, R. Metzler, and T.F. Nonnenmacher, Phys. Rev. E **55**, 99 (1997); S. Jespersen, R. Metzler, and H.C. Fogedby, *ibid.* **59**, 2736 (1999).
- [13] R. Gorenflo and F. Mainardi, in *Fractals and Fractional Calculus in Continuum Mechanics*, edited by A. Carpinteri and F. Mainardi (Springer Verlag, Vienna, 1997); Report No. A-14/96 (unpublished).
- [14] UA5 Collaboration, G.J. Alner *et al.*, Phys. Rep. **154**, 247 (1987).
- [15] SLD Collaboration, K. Abe *et al.*, Phys. Lett. B **371**, 149 (1996).
- [16] H1 Collaboration, S. Aid *et al.*, e-print hep-ex/9608011.